

Accelerating Compressed Sensing in Cartesian Parallel Imaging Reconstructions using an Efficient and Effective Circulant Preconditioner

Jeroen van Gemert¹, Kirsten Koolstra², Peter Börner³, Andrew Webb², and Rob Remis¹

¹*Circuits and Systems Group, Delft University of Technology, Delft, Netherlands*, ²*C.J. Gorter Center for High-Field MRI, Leiden University Medical Center, Leiden, Netherlands*, ³*Philips Research Hamburg, Hamburg, Germany*

Synopsis

Reconstruction methods in parallel imaging and compressed sensing problems are generally very time consuming, especially for a large number of coil elements. In this work, the image is reconstructed using the Split Bregman algorithm (SB). We present an efficient and effective preconditioner that reduces the number of iterations in the linear least squares step of SB by almost a factor of 5 as alternative to extra variable splitting. The designed preconditioner works for Cartesian sampling schemes and for different coil configurations. It has negligible initialization time and leads to an overall speedup factor of 2.5.

Introduction

High undersampling factors can be achieved by using Parallel Imaging (PI) and Compressed Sensing (CS)¹⁻⁶. We use the Split Bregman algorithm (SB) to reconstruct the image in which solving a linear least squares problem, usually solved iteratively, is the most time-consuming part⁷. In Cartesian sampling, however, this part can be solved directly by using extra variable splitting^{8,9}. Alternatively, the number of iterations can be reduced by using preconditioners, although in literature they either have high initialization costs due to patient-specific coil sensitivities¹⁰, or evaluation of the preconditioner is expensive¹¹⁻¹³. In this work, we propose an efficient and accurate Fast Fourier Transform (FFT)-based preconditioner for Cartesian PI-CS reconstructions that takes the coil sensitivities on a patient-specific basis into account and has negligible initialization time. Our imaging results show that the proposed preconditioner framework provides a good starting point for accelerating non-Cartesian reconstructions.

Theory

For each SB iteration a linear least squares problem of the form $\mathbf{A}\mathbf{x} = \mathbf{b}$ has to be solved, where \mathbf{x} is the true image, \mathbf{b} is the weighted undersampled k-space data, and

$$\mathbf{A} = \mu \sum_{i=1}^{N_c} (\mathbf{RFS}_i)^H \mathbf{RFS}_i + \lambda (\mathbf{D}_x^H \mathbf{D}_x + \mathbf{D}_y^H \mathbf{D}_y) + \gamma \mathbf{W}^H \mathbf{W} \quad (1)$$

is the system matrix that remains constant throughout the SB iterations. Here, the \mathbf{S}_i are diagonal matrices representing complex coil sensitivity maps for each of the N_c channels. Furthermore, \mathbf{F} is the discrete two-dimensional Fourier transform matrix, and the undersampling pattern is specified by the binary diagonal sampling matrix \mathbf{R} . The regularization parameters λ and γ in (1) are promoting sparsity via the total variation constraint (employing differentiation matrices \mathbf{D}_x and \mathbf{D}_y) and the unitary wavelet transform \mathbf{W} , respectively.

The second and third term in (1) are block circulant with circulant blocks (BCCB) matrices and are diagonalized by the Fourier matrix \mathbf{F} . Writing

$$\mathbf{A} = \mathbf{F}^H \mathbf{F} \mathbf{A} \mathbf{F}^H \mathbf{F} = \mathbf{F}^H \mathbf{K} \mathbf{F}$$

we have

$$\mathbf{K} = \underbrace{\mu \sum_{i=1}^{N_c} \mathbf{FS}_i^H \mathbf{F}^H \mathbf{R}^H \mathbf{RFS}_i \mathbf{F}^H}_{\mathbf{K}_c} + \underbrace{\lambda \mathbf{F} (\mathbf{D}_x^H \mathbf{D}_x + \mathbf{D}_y^H \mathbf{D}_y) \mathbf{F}^H}_{\mathbf{K}_d} + \underbrace{\gamma \mathbf{I}}_{\mathbf{K}_w}$$

where \mathbf{K}_d and \mathbf{K}_w are diagonal, but \mathbf{K}_c is not. Most of the energy in \mathbf{K}_c is located around its main diagonal, however. Hence, we approximate the matrix \mathbf{K}_c by its diagonal to arrive at a BCCB approximation of \mathbf{A} as preconditioner for solving the linear system. The required steps can be efficiently performed using FFTs.

Methods

MR Data Acquisition: A Philips Ingenia 3T dual transmit MR system was used to acquire *in vivo* data. A 12-element posterior receiver array and 15-channel head coil were used for reception in spine and brain, respectively, whereas the body coil was used for RF transmission. T_1 -weighted images were acquired using a standard clinical TSE sequence and IR-TSE sequence for spine and brain, respectively.

Reconstruction: The SB algorithm was implemented in MATLAB on a standard Windows 64-bit PC with 8 GB of internal memory. Unprocessed k-space data was stored per channel and used to construct cropped complex coil sensitivity maps¹⁴. Both the individual coil images and the coil sensitivity maps were normalized. Reconstruction for the spine data set was performed without and with coil compression^{15,16}. A random line pattern and a fully random pattern, both with variable density, were studied for undersampling factors four ($R=4$) and eight ($R=8$).

Results

Figure 1 shows the TSE spine images for Cartesian undersampling factors $R=4$ and $R=8$. The full system matrix is constructed for illustration purposes only and compared with its circulant approximation in Fig. 2.

Figure 3a shows the number of iterations required for the preconditioned conjugate-gradient (PCG) solver to converge in each SB iteration without preconditioner, with the Jacobi preconditioner (the diagonal of matrix A), and with the circulant preconditioner proposed in this abstract. The reduced number of iterations leads to a shortened reconstruction time, plotted in Fig. 4a for the total PCG part in the SB algorithm (4.65x), and in Fig. 4b for the entire reconstruction algorithm (2.5x). For all matrix sizes the initialization time of the preconditioner is less than 2% of the image reconstruction time. Similar results are obtained for the 15-channel head coil as shown in Fig. 5.

Discussion and Conclusion

We have presented a circulant preconditioner that reduces the reconstruction times considerably for Cartesian CS-PI problems by solving the least-squares problem in the SB algorithm almost 5 times faster than without preconditioning, resulting in an overall reconstruction speedup factor of about 2.5. Without loss of performance it supports further speed up through coil compression, and works well for different coils and undersampling factors. The preconditioner has negligible initialization and evaluation time and is therefore highly scalable. In future work, our method will be compared in performance to extra variable splitting and extended to non-Cartesian sampling where direct solution methods are no longer feasible, possibly leading to faster reconstruction times.

Acknowledgements

We would like to thank Ad Moerland from Philips Healthcare Best (The Netherlands) and Mariya Doneva from Philips Research Hamburg (Germany) for helpful discussions on reconstruction.

References

1. Pruessmann K et al. SENSE: Sensitivity Encoding for Fast MRI. *Magnetic Resonance in Medicine*, 1999; 42(5):952-962.
2. Griswold M et al. Generalized Autocalibrating Partially Parallel Acquisitions (GRAPPA). *Magnetic Resonance in Medicine*. 2002; 47(6):1202-1210.
3. Blaimer M et al. SMASH, SENSE, PILS, GRAPPA: How to Choose the Optimal Method. *Topics in Magnetic Resonance Imaging*. 2004; 15(4):223-236.
4. Deshmane A et al. Parallel MR imaging. *Journal of Magnetic Resonance Imaging*. 2012; 36(1):55-72
5. Donoho D et al. Compressed Sensing. *IEEE Transactions on Information Theory*. 2006; 52(4):1289-1306.
6. Lustig M et al. Sparse MRI: The Application of Compressed Sensing for Rapid MR Imaging. *Magnetic Resonance in Medicine*. 2007; 58(6):1182-1195
7. Goldstein T et al. The split Bregman Method for L1-Regularized Problems. *SIAM Journal on Imaging Sciences*. 2009; 2(2):323-343.
8. Ramani A et al. Parallel MR Image Reconstruction using Augmented Lagrangian Methods. *IEEE Trans Med Imaging*. 2011;30(3):694-706.
9. Weller D et al. Augmented Lagrangian with Variable Splitting for Faster Non-Cartesian L1-SPIRiT MR Image Reconstruction. *IEEE Trans Med Imaging*. 2014;33(2):351-361.
10. Saad Y. Iterative methods for sparse linear systems. *Society for Industrial and Applied Mathematics*. 2003; 2.
11. Chen C et al. Real Time Dynamic MRI with Dynamic Total Variation. *International Conference on Medical Image Computing and Computer-Assisted Intervention*. 2014;138-145
12. Li R et al. Fast Preconditioning for Accelerated Multi-contrast MRI Reconstruction. *International Conference on Medical Image Computing and Computer-Assisted Intervention*. 2015;700-707.
13. Xu Z et al. Efficient Preconditioning in Joint Total Variation Regularized Parallel MRI Reconstruction. *International Conference on Medical Image Computing and Computer-Assisted Intervention*. 2015;563-570.
14. Uecker M et al. ESPIRiT - An Eigenvalue Approach to Autocalibrating Parallel MRI: Where SENSE Meets GRAPPA. *Magnetic Resonance in Medicine*. 2014; 71(3):990-1001.
15. Huang F et al. A Software channel compression technique for faster reconstruction with many channels. *Magnetic Resonance Imaging*. 2008; 26(1):133-141.
16. Zhang T et al. Coil Compression for Accelerated Imaging with Cartesian Sampling. *Magnetic Resonance in Medicine*. 2013; 69(2):571-582.

Figures

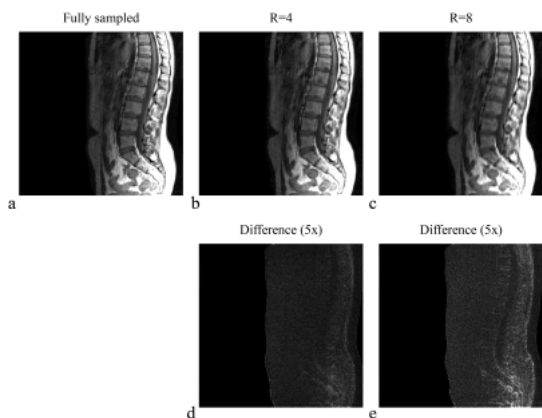


Figure 1: Reconstruction results for a T_1 -weighted spine scan using different Cartesian undersampling factors. (a) shows the fully sampled scan as a reference, whereas (b) and (c) depict the reconstruction results for undersampling factors four ($R=4$) and eight ($R=8$), respectively. The absolute difference is shown in (d) and (e) for $R=4$ and $R=8$, respectively. The reconstruction matrix is 512×512 . Regularization parameters were set to $\mu = 1 \cdot 10^{-3}$, $\lambda = 4 \cdot 10^{-3}$, and $\gamma = 1 \cdot 10^{-3}$. Images were acquired using a TSE sequence with $FOV = 340 \times 340 \text{ mm}^2$; in-plane resolution $0.66 \times 0.66 \text{ mm}^2$; slice thickness = 4 mm, $TE/TR/TSE \text{ factor} = 8 \text{ ms}/648 \text{ ms}/8$.

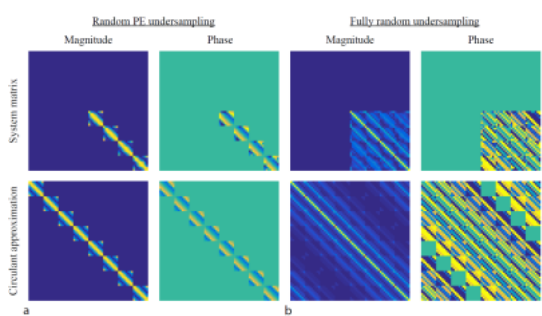


Figure 2: System matrix and its circulant approximation. The first two columns and the last two columns show the system matrix elements for random Phase-Encoding (PE) (a) and fully random (b) undersampling, respectively. The top row depicts the elementwise magnitude and phase of the true system matrix A , whereas the bottom row depicts the elementwise circulant approximation. The zeros in A are not present in the circulant approximation, since the circulant property is enforced. The newly introduced entries do not add relevant information as the image vector on which the system matrix acts contains zero signal in the corresponding region.

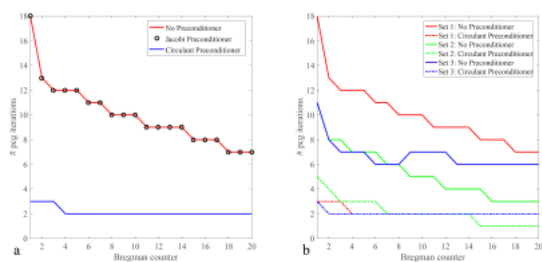


Figure 3: Number of PCG iterations required in each Split Bregman iteration. The circulant preconditioner reduces the number of iterations considerably compared with the non-preconditioned case. The Jacobi preconditioner hardly reduces the number of PCG iterations. (a) depicts the number of PCG iterations for Set 1: $\mu = 1 \cdot 10^{-3}$, $\lambda = 4 \cdot 10^{-3}$, $\gamma = 1 \cdot 10^{-3}$, whereas (b) depicts the number of PCG iterations for Set 1, Set 2: $\mu = 1 \cdot 10^{-2}$, $\lambda = 4 \cdot 10^{-3}$, $\gamma = 1 \cdot 10^{-3}$, and Set 3: $\mu = 1 \cdot 10^{-3}$, $\lambda = 4 \cdot 10^{-3}$, $\gamma = 4 \cdot 10^{-3}$. The preconditioner shows the largest speed up factor when the regularization parameters are well-balanced.

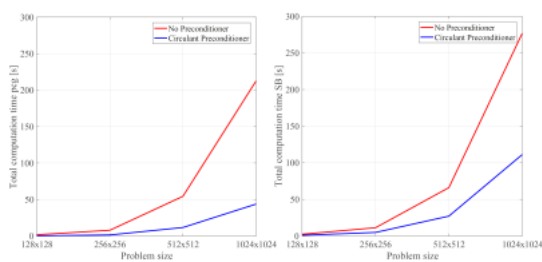


Figure 4: Computation time for 20 Split Bregman iterations and different problem sizes. (a) Using the preconditioner, the total computation time for the

PCG part in 20 Bregman iterations is reduced by a factor larger than 4.5 for all studied problem sizes. (b) The computation time for 20 Split Bregman iterations of the complete algorithm (including Split Bregman updating steps) is reduced approximately by a factor of 2.5 for the considered problem sizes.

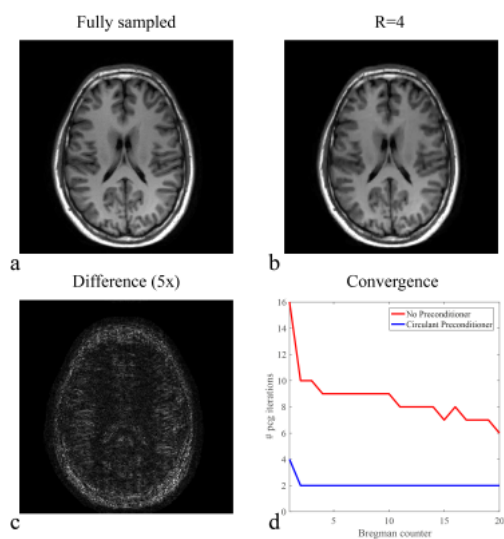


Figure 5: Reconstruction results for a T_1 -weighted brain scan. (a) shows a fully sampled scan as a reference and (b) the reconstruction results for an undersampling factor $R=4$. The absolute difference is shown in (c). The reconstruction matrix has dimensions 256×256 and regularization parameters where chosen as $\mu = 1 \cdot 10^{-3}$, $\lambda = 4 \cdot 10^{-3}$, $\gamma = 2 \cdot 10^{-3}$. The convergence results for the PCG part with and without preconditioner are plotted in (d). Images were acquired using an IR TSE sequence with FOV = 230×230 mm²; in-plane resolution 0.90×0.90 mm²; slice thickness = 4 mm; TE/TR/TSE factor = 20ms/2000ms/8; refocusing angle = 120° ; IR delay: 800ms.